Spin Glass Behaviour of Magnetic Carbon Nanoclusters

A. V. Rode[*], A. G. Christy[**], N. R. Madsen[*], E. G. Gamaly[*], B. Luther-Davies[*],
D. Arčon[***],[****], A. Zorko[***], Z. Jaglicic[***]

[*]Laser Physics Centre, Research School of Physical Sciences and Engineering, and
[**]Department of Earth and Marine Science, Faculty of Science, andyc@ems.anu.edu.au
The Australian National University, Canberra, Australia, avr111@rsphysse.anu.edu.au
[***]Faculty of Mathematics and Physics, University of Ljubljana, Slovenia,
[****]Institute Jozef Stefan, Ljubljana, Slovenia, denis.arcon@ijs.si

ABSTRACT

Carbon nanoclusters produced by high-repetition-rate laser ablation of graphite and glassy carbon in Ar exhibits para- and ferromagnetic behavior at low temperature. Magnetic susceptibility and electron paramagnetic resonance of carbon nanofoam samples produced at different Ar pressures demonstrate ferromagnetic behaviour at low temperatures. The results show that the degree of remanent order is strongly dependent on the magnetic history, i.e. whether the samples were cooled under zero-field or field conditions. Such behaviour is typical for a spin glass picture where the system can exist in many different roughly equivalent spin configurations. Detailed EPR studies identified three different types of independent spin systems with relaxation times 100 ns, 0.1-1 µs, and 1 ms. We conclude that unpaired spins exist in the nanofoam in three quite different structural environments. Their role in the magnetic ordering is discussed.

Keywords: magnetic carbon nanoclusters, ferromagnetic carbon, spin glass

1   INTRODUCTION

The discovery of ferromagnetic response in polymerized C_{60} forms [1] and cluster-assembled carbon nanofoam [2] opens new possibilities to throw some additional light on the carbon-based ferromagnetism. Carbon nanofoam is synthesized by laser-ablation of a graphite or glassy carbon target in an argon atmosphere [3,4]. Electron diffraction of the nanofoams suggests the presence of hyperbolic "schwarzite" layers [3,5]. "Schwarzite" layers are saddle-shaped graphitic layers in which the negative Gaussian curvature arises from the presence of carbon rings larger than six members. The carbon nanofoam shows strong magnetization immediately after the synthesis; most of this is lost on a time scale of several minutes immediately after the synthesis, but a fraction of the magnetization is stable even on a very long time scale. A saturation magnetization of $M_s = 0.42$ emu/g at 1.8 K can be measured even 12 months after synthesis [2]. Here we present the results of a systematic study of magnetic susceptibility and electron paramagnetic resonance (EPR) of carbon nanofoam samples produced at different Ar pressures, conducted with the aim of elucidating the nature and ordering behavior of the spin centers in the carbon nanofoam.

2   EXPERIMENTS

The carbon nanofoam samples were analysed by continuous-wave (cw) and pulsed EPR techniques, and the results were correlated to the dc magnetization data.

2.1   Laser Ablation Conditions

Carbon nanofoam samples were prepared using high power frequency doubled $Nd:YVO_4$ laser operating at the second harmonic (532 nm), with repetition rate 1.5 MHz, pulse duration 12 ps [6], and focused down to a spot size ~15 µm. This gave a maximum incident intensity of 7×10^{11} W/cm^2 with corresponding fluence 8.6 J/cm^2. The ablated mass per pulse was of the order of 10^{-10} g which corresponds to ~0.3 mg/s. To avoid crater formation on the target surface and provide steady state ablation conditions, the laser beam was scanned using a constant velocity spiral pattern formed by x-y scanning mirrors. The laser beam was moved at a velocity of 1 m/s (10 laser pulses per spot) over the target surface. To produce the samples of this study, graphite and glassy carbon targets were ablated in a stainless steel vacuum chamber pumped to a base vacuum of 5×10^{-7} Torr, and then filled with high-purity (99.995%) Ar gas at various pressures in the range 0.2 Torr – 200 Torr.

2.2   Impurity Analysis

An impurity analysis of the carbon nanofoam samples made in different conditions was performed using inductively coupled plasma-atomic emission spectroscopy (ICP-AES). Samples were digested in a small volume of hot concentrated nitric acid and then diluted to a dilution factor of ca. 1:100 using ultra-pure water. The concentrations of each element measured were calculated from the intensities of specified atomic emission lines relative to those in blank 2% nitric acid and in a multi-element standard prepared from commercial standard solutions. Effective detection limits in the foam ranged from hundreds of ppb for $3d$ transition metals, lanthanides and Mg to several ppm for Na, K, Ca and B-group metals including Al.

The sum of all the impurity elements analyzed in the foam samples of this study was ~600-900 ppm, the dominant impurity elements in the samples were Ca (300-700 ppm); Na (64-137 ppm); K (10-54 ppm); Zn (23-92 ppm), Cu (6-14 ppm), Ni (25-37 ppm) and Fe (64-174 ppm). The measured impurity concentration together with the magnetization and EPR data confirm that the observed magnetic behaviour cannot arise from ferromagnetic impurities but rather is an intrinsic property of the nanofoam.

2.3 Structural Characterisation

The HRTEM was performed using a JEOL-3000F field emission electron microscope operated at 300 kV with maximum resolution 1.7 Å. Fourier transforms of some images with diffraction rings in the range 4 – 5Å expected for Schwarzite-type curved sheets. However, more systematic study is required to find a correlation between the nanofoam properties and the schwartzite-like periodicity within the clusters.

EELS spectra where collected from both the carbon K-edge (280-350 eV) and the low loss (0-50 eV) regions. The fraction of sp^3 bonded carbon atoms was calculated from the carbon K-edge [7] assuming that $(sp^2 + sp^3) = 100\%$. The sp^3 content was found to be in the range 8 – 20%. There was no clear dependence of the proportion of sp^3 bonding or the cluster size on the Ar pressure in the experiments. The low loss region contains plasmon loss peaks, which were used to approximate the volume density [8]. The individual cluster density was found to be in the range 1.55 – 1.90 g/cm^3, which is close to our earlier estimate of 1.9 g/cm^3 [3].

2.4 Magnetisation and EPR measurements

DC magnetic susceptibilities measurements are summarized in Fig. 1. In all experiments we applied the same cooling protocol: first measurement was taken after zero-field cooling (ZFC) to 2 K and in the second run the measurements were taken under field-cooled (FC) conditions.

Direct current (dc) magnetization measurements were performed on a Quantum Design SQUID magnetometer in a magnetic field of 100 Oe down to a temperature of 2 K.

All samples show very large field-cooling dependence below room temperature: $\chi(T)$ is larger under FC conditions when compared to values measured under ZFC conditions.. While field-cooled dependences typically show monotonic increase of the magnetic susceptibility with decreasing temperature, the zero-field data have a maximum at 50 - 300 K and decrease again below that temperature; this behaviour is characteristic of spin glasses [9].

All samples show weak hysteresis in the field curves at low temperature. A very steep increase in the magnetic moment when cycling with a field around 0 Oe is a clear signature of the magnetic ordering in these samples. We note that this behavior gradually disappears with increasing temperature and is barely discernible at room temperature.
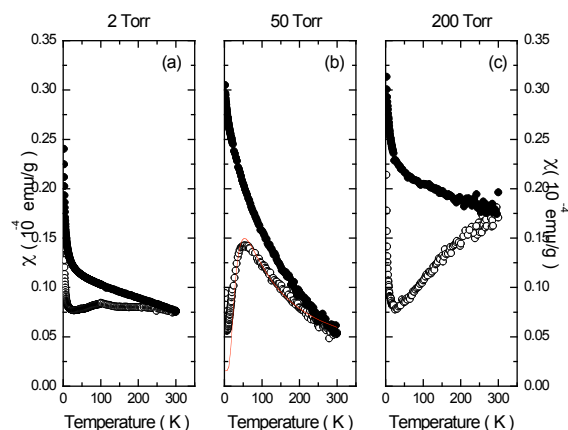

Fig. 1. A temperature dependence of ZFC (open circles) and FC (solid circles) dc magnetic susceptibilities for different carbon nanofoam samples at various Ar pressure.

3 DISCUSSION

We distinguish three types of temperature behavior, each of which was encountered in several carbon-nanofoam samples. Based on our magnetization measurements we can conclude that carbon nanofoam samples studied in this work:

(i) Show nonzero remanent magnetization at low temperatures, evidenced by the hysteresis curves. Saturation magnetization was estimated to be 0.35 emu/g at T=2 K, i.e. a value, that is very close to one measured in [2]. Taking a measured concentration of Fe particles 150 ppm and saturation magnetization for a typical iron oxide Fe2O3 (80 emu/g), one can estimate the upper limit for the impurity contribution to be no more than 0.012 emu/g. We thus conclude that the measured magnetic properties are characteristic of carbon nanofoam.

(ii) The degree of remanent order is strongly dependent on the magnetic history, i.e. whether the samples were cooled under zero-field or applied field conditions.

(iii) Such remanence effects are consistent with a spin glass, in which the system can exist in many roughly equivalent spin configurations rather than one unique long-range ordered scheme. The spin-freezing temperature is unusually high (50 - 300 K) compared with ≤ 15 K for typical spin glasses [9]. The maximum in the zero-field magnetic susceptibility experiments and their field dependence indicate that there is competition between ferromagnetic and antiferromagnetic exchange pathways, accounting for the spin glass behavior and/or a low-dimensionality of the system.

(iv) A rapid increase in susceptibility at very low T implies that some spins remain unfrozen at T_f and do not couple strongly at all, thus showing a near-zero T_c. The complexity of T-χ behavior therefore suggests that the nanofoam contains at least two distinct types of spin-bearing region, one with frustrated coupling and one with negligible coupling.

EPR measurements were performed on a commercial Bruker E580 spectrometer. Continuous wave (cw) measurements were done on a Varian dual resonator and Oxford continuous flow ESR 900 cryostat. Pulsed EPR experiments were on the other hand performed using a Bruker dielectric resonator, ER 4118X-MD5. A typical $\pi/2$ pulse length used in our experiments was 16 ns. For the relaxation studies, inversion-recovery technique was applied with signal detection either via free-induction decay or echo signal. In all experiments we used appropriate phase cycling sequences to remove unwanted signals.

Samples prepared under different Ar atmospheres had similar but rather complex cw EPR lineshapes. Pulsed EPR measurements resolved at least three different centers in all carbon nanofoam samples with the characteristic room temperature g-factors 2.0036, 2.0031 and 2.0016. The intensity of each individual center depends not only on sample characteristics but also on thermal history. The relative proportion of the $g = 2.0016$ and $g = 2.0036$ lines changed systematically on going from samples prepared at 2 Torr to 50 Torr Ar atmosphere (Fig. 8). The narrow $g = 2.0016$ line gradually lost intensity with increasing Ar pressure, and in samples prepared at high pressure only the $g = 2.0036$ line could be seen (Fig. 2).

The data imply a very inhomogeneous ground state of carbon nanofoams with at least three different types of center. The main center has a g-factor 2.0031 and is responsible for the central part of the cw EPR spectrum and can be also seen in free induction decay experiments. The other two centers are likely responsible for the background of the cw EPR line and can be only distinguished in echo experiments.
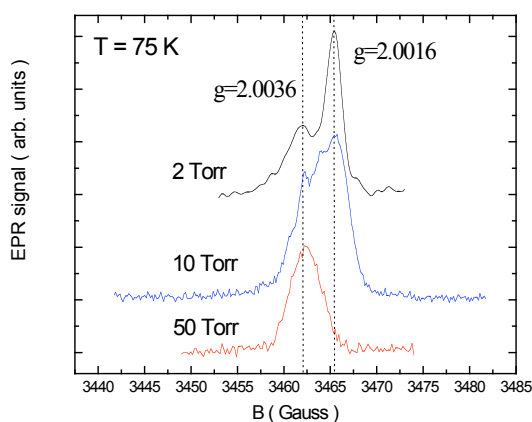

Fig. 2. A variation of the field-sweep EPR spectra measured at 75 K in samples prepared under different Ar atmosphere.

We bore in mind the possibility that the spins are due to magnetic impurities. The most likely candidates would be different iron compounds, in particular iron oxide or iron carbide particles. We stress that the total analysed Fe is so low that even if all the iron was in such compounds, we would have difficulties in observing the signals due to sen-

sitivity problems. Our EPR experiments do not detect any non-carbon magnetic impurity in carbon nanofoam samples.

We note that all three g-factor values are reasonable for carbon-based defects, but may correlate with different structure/bonding environments. A g-factor of ca. 2.0030-2.0045 is characteristic of spins in polymeric/diamond-like systems with substantial sp^3 character in the C-C bonds [10-12]. The two spin types with high g-factors may correspond to radical carbons in such a bonding environment. The value $g = 2.0016$ is very low for carbon; g-factors less than the free-electron value ($g_e = 2.00232$) are typical for carbons in near-planar sp^2-like environments such as fullerenes, which is presumably the case for these centers.

In an attempt to shed some additional light on the contributions of the three centers to the observed magnetism, we measured spin-lattice relaxation times t_1 on different samples. Results are summarized in Fig. 3.
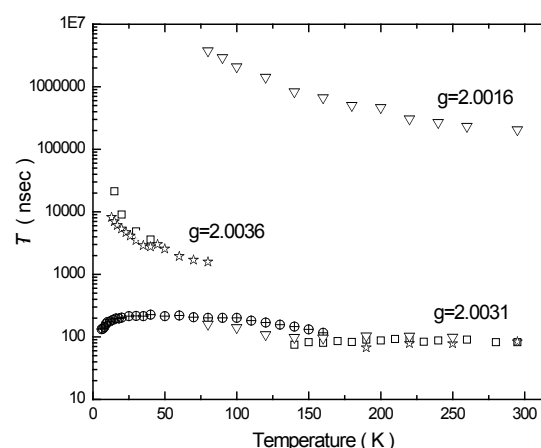

Fig. 3. A temperature dependence of the electron spin-lattice relaxation times measured in different carbon nanofoam samples. Here (∇) stands for experiments on 2 Torr sample, ($\star$) for 10 Torr, ($\oplus$) for 50 Torr , and finally ($\square$) for 200 Torr experiments.

We first note that all centers have very different relaxation times, which differ by orders of magnitude. This supports the conclusion that they correspond to unpaired spins in quite different structural environments. The narrow component with g-factor = 2.0031 has the shortest t_1 of the order of several 100 ns, the low temperature signal at 2.0036 has t_1 in the range of several 10 μs while g=2.0016 signal has t_1 of the order 200 μs already at room temperature (at low temperatures it becomes several ms and thus difficult to measure). Such different t_1 values prove that these centers are not capable of establishing common spin temperature; in other words they do not interact significantly with each other. Therefore, they can be regarded as three independent spin systems.

The very long spin-lattice relaxation time of the $g = 2.0016$ line suggests that the local field dynamics in this

part of the sample is strongly suppressed. Defects associated with this line should be very diluted and hence cannot contribute to any sort of magnetic phenomena. However, note that decrease in temperature is observed to cause replacement of the $g = 2.0016$ resonance by the $g = 2.0036$, with a relaxation time nearly four orders of magnitude shorter. We speculate on the basis of the observed transfer of EPR intensity between $g = 2.0016$ and $g = 2.0036$ lines that these two centers have a similar spatial location. The crossover between the two resonance types can be seen in Fig. 3, and occurs at about the temperature of the susceptibility maximum.

From the structure-g correlation noted above, we deduce that the transformation from a low-g to a high-g state is likely due to change in the bonding geometry of the carbon carrying the unpaired spin. Our higher g-factor signals arise from sample regions with more sp^3 character. On cooling, a transition occurs in which the spins shift from low-g, "sp^2-like" centers in the carbon sheet to nearby higher-g environments that are more "sp^3-like"; the rearrangement of the bonding electrons that is involved may either cause relocation of the unpaired spin to a more buckled part of the sheet, or may cause buckling of the sheet without relocation of the spin. In either case, the shorter relaxation time in the non-planar environment then allows a frustrated mixture of ferro- and antiferro- couplings between spins that reduces the low-T susceptibility. The $g = 2.0031$ resonance with very short relaxation time is present at T above and below this transition (Fig. 3): these may also couple to the $g = 2.0036$ spins and facilitate glass formation. The low-T Curie tail seen in the χ-T plots cannot be exclusively correlated with any of the three center types detected by EPR spectroscopy.

4 CONCLUSION

In conclusion, all samples showed magnetic cooperative phenomena at low temperatures. Magnetic susceptibility data shows large differences between ZFC and FC experiments that are consistent with formation of a spin glass with unusually high freezing temperature, exceeding room temperature in one sample. There is an additional paramagnetic component in the material that gives a Curie law-like increase in χ at very low T. Magnetic inhomogeneity is supported by detailed EPR studies, where we recognized three different types of center. One type has a g-factor 2.0016 and a very long relaxation time of the order of 1 ms, which renders it unlikely to participate in magnetic ordering. However reduction in temperature of the sample, or increase of the gas pressure of synthesis, cause this center to be replaced by a different type with $g = 2.0036$, t_1 of the order of 0.1 - 1 µs. The transition between these occurs at T similar to that where the spin glass susceptibility maximum is observed. Hence, coupling of these centers may be vital for the freezing of spins. The third type have $g = 2.0031$ and ca. 100 ns relaxation time, is present at all temperatures, and may facilitate coupling. The higher g-factors (>

2.003) are typical of amorphous carbon systems with significant sp^3 character, i.e. strongly non-planar parts of a carbon sheet.

REFERENCES

[1] T. L. Makarova, B. Sundqvist, R. Höhne, P. Esquinazi, Y. Kopelevich, P. Scharff, V. Davydov, L. S. Kashevarova, and A. V. Rakhmanina, *Nature* **413**, 716 (2001).

[2] A. V. Rode, E. G. Gamaly, A. G. Christy, J. G. Fitz Gerald, S. T. Hyde, R. G. Elliman, B. Luther-Davies, A. I. Veinger, J. Androulakis, and J. Giapintzakis, *Phys. Rev.* **B 70**, 054407 (2004).

[3] A. V. Rode, S. T. Hyde, E. G. Gamaly, R. G. Elliman, D. R. McKenzie, and S. Bulcock, *Appl. Phys. A* **69**, S755 (1999).

[4] A. V. Rode, E. G. Gamaly, and B. Luther-Davies, *Appl. Phys. A* **70**, 135 (2000).

[5] A. V. Rode, R. G. Elliman, E. G. Gamaly, A. I. Veinger, A. G. Christy, S. T. Hyde, B. Luther-Davies, *Appl. Surf. Sci.* **197-198**, 644 (2002).

[6] B. Luther-Davies, V. Z. Kolev, M. J. Lederer, N. R. Madsen, A. V. Rode, J. Giesekus, K.-M. Du, and M. Duering, *Appl. Phys. A* **79**, 1051-1055 (2004).

[7] D. D. Berger, D. R. McKenzie, and P. J. Martin, *Philos. Mag. Lett.* **57**, 285 (1988).

[8] R. F. Egerton, "Electron Energy-Loss Spectroscopy in the Electron Microscope", 2nd edition Plenum Press, New York, 1996.

[9] K.H. Fischer and J.A. Hertz, "Spin Glasses", Cambridge University Press, Cambridge, 1991.

[10] A. Sadki, Y. Bounouh, M. L. Theye, J. von Bardeleben, J. Cernegora, and J .L. Fave, *Diamon. Rel. Mater.* **5**, 439 (1996).

[11] Collins, R.C. Barklie, J.V. Anguita, J.D. Carey, and S.R.P. Silva, *Diamond Relat. Mater.* **9**, 781 (2000).

[12] J. Ristein, J. Schöfer, and L. Ley, *Diamond Relat. Mater.* **4**, 508 (1995).